A study on Growing of Ice Crystal after Breaking of Super Cooling Condition by Numerical Simulations and MRI Measurements

Translated Paper

Transactions of the Japan Society of Refrigerating and Air Conditioning Engineers, Vol.34,No.1(2017),pp.57-60, Received date: January 27, 2017

A study on Growing of Ice Crystal after Breaking of Super Cooling Condition by Numerical Simulations and MRI Measurements

[Original: Trans. JSRAE, Vol.33, No.3, pp.261-266,(2016)]

Rika KOBAYASHI[*¶] Arlyn Dublin MACASERO[**¶] Shingo MATSUKAWA[**†]

*College of Bioresource Science, Nihon University
(1866, Kameino, Fujisawa city, Kanagawa Prefecture, 252-0880)
** Department of Food Science and Technology, Tokyo University of Marine Science and Technology,
(4-5-7, Konan, Minato-ku, Tokyo, 108-8477)

Summary

Numerical simulations and magnetic resonance imaging (MRI) measurements have been carried out for a better understanding of the behavior in ice crystal growing after breaking of super cooling condition in aqueous solutions. The numerical simulations showed that a fast cooling from outside caused ice nucleation from the outer edge and the expansion of bulky ice crystal, on the other hand, a slow cooling showed ice nucleation from inside and expansion of fibrous ice crystal. Temperature measurements and MRI measurements for a phantom test sample with cylindrical double layer structure showed that frisky ice crystals were outbreak throughout the outer layer inducing the temperature increase up to 0 degree after the breaking of super cooling condition and the inner layer stayed as a liquid at the lower temperature, and after that, bulk ice crystals were expanded from the surface of the inner part in outer layer causing the increase of temperature of inner part.

Keywords: Ice crystallization, Super cooling condition, Numerical simulation, MRI

1. Introduction

Freezing time, size and shape of ice crystals, generation site of ice nuclei are important factors to be considered to impart high quality thawing in frozen food products. In food freezing process, ice crystal formation can cause physical and biochemical stress in frozen food which can affect its sensory evaluation after thawing[1]. Physical stress refers to osmotic stress, which is caused by the formation and expansion of ice inside a cell structure. For instance, ice crystals formation in plant tissue destroyed the vacuoles caused by volume expansion and dehydration[2] and cell structure collapses as the permeability of the cell membrane is increased[3]. On the other hand, biochemical stress refers to various chemical reactions such as auto-oxidation and reactions involving enzymes that occurred during the freezing process. Examples include the browning of tuna flesh[4], lipid oxidation[5] etc. during the storage stage in food freezing.

Thaw recovery properties of the gelled food products are highly dependent on the characteristics of the resulting ice crystals. In gel-like food products such as tofu and konjac, the existing network structure is frozen and destroyed by the volume expansion of the ice crystal. When a new network structure is formed, gel matrix compressed between the ice crystals and results to quality degradation such as texture destruction and reduction of water retention ability [6)7)]. The size and shape of ice crystals are determined in 2 factors namely: (1) ice crystal nucleation frequency and ice crystal growth rate, (2) the freezing rate used as their indicator. Food freezing is treated at temperature range between -80^{0}C and 0^{0}C. At lower refrigerant temperature, the higher the frequency of nucleation thus, the slower ice crystal growth rate. Therefore, the higher the freezing rate, the more nuclei are generated, resulting to formation of more fine ice crystals qualitatively[8]. Quantitative descriptions of freezing rate and size of ice crystal in food have also been obtained experimentally[9)10)]. Furthermore, much attention is given to food freezing techniques that aim to increase the nucleation frequency of finer ice crystals. Controlling the nucleation frequency by using ice nucleation products, ultrasound, high pressure, etc. results to the generation of finer ice crystals[11]. Similarly, utilizing the fact that nucleation frequency increases due to super cooling phenomenon, a freezing method for the generation of finer ice crystals has been studied[12)13)14)]. For example, finer ice crystals are formed in tofu and collagen gel samples, maintained at the super cooled state, after breaking the super cooling condition rather than samples frozen at similar freezing rates. When utilizing the super cooling phenomenon, the size and number of ice crystals formed depending on the degree of super cooling since nucleation frequency also increases as the degree of super cooling increases. It has been

†Fax:+81 3-5463-0581 E-mail: matsukaw@kaiyodai.ac.jp

¶KOBAYASHI and MACASERO contributed equally to this work.

clarified that a freezing method that utilizes the super cooling phenomenon can form finer and isotropic ice crystal structures. However, there are still many points left unclear with regards to ice crystal growth process after nucleation[15].

In this research, we conducted numerical simulations and nuclear magnetic resonance (MRI) to understand the growth behavior of ice crystals after breaking the super cooling condition, which is an important issue in freezing method that utilizes the super cooling phenomenon.

2. Methodology

2.1 Numerical Simulation

The growth behavior of ice crystals was simulated using a 2-dimensional lattice model consisting of 60x90 cells with the length of h. With the initial outer lattice temperature set at 0°C, ice crystal, temperature and solute concentration distributions were obtained at cooling rates equal to 0.05 °C/τ and 0.01 °C/τ, where τ is the time of every iterative calculation. The initial concentration of solute was 1% and the freezing point depression was 1 °C per 1%. The breaking temperature of super cooling condition for each cell was generated by the normal random number with an average of -10 °C and a standard deviation of 3 °C. The heat diffusion D_h was $0.1h^2/\tau$ and the molecular diffusion of solute was 0.002 h^2/τ. Heat capacity of water was 4.2J/K/g, and heat of solidification and heat capacity of ice were 336J/g and 2.52J/K/g, respectively, which were considered to be constant against temperature changes. Simulations were carried out by a homemade program written by Mathematica10 (Wolfram Research Inc., Illinois).

2.2 MRI Measurement

2.2.1 Sample

A test sample (phantom) with a double layer cylindrical structure was used for MRI measurements. It was fabricated using a PE bottle as an outer layer with diameter and height equal to 78 mm and 140 mm, and a smaller PE bottle as an inner layer with diameter and height equal to 26 mm and 120 mm, respectively. Both inner and outer layers were filled with 0.3% of κ–carrageenan (MRC polysaccharide, Tokyo) and 0.05 % $CuSO_4$ solution.

2.2.2 Method

Measurements of the phantom were performed using MRTe.300V (MR Technology, Tsukuba) with magnetic field strength of 0.3 T. The pulse sequence was set to multi-slice spin-echo method with pulse sequence echo time of 21 ms and repetition time of 325 ms. Prior to MRI measurement, the phantom was immersed in a low temperature liquid bath at -8 °C for 3 hours to attain super cooling condition in both inner and outer layers, and then, the phantom was placed in the sample chamber at room temperature to perform MRI measurements.

3. Results and Discussions

3.1 Numerical Simulation

The effect of cooling rate in the behavior of ice crystal growth after breaking the super cooling condition was studied using numerical simulation. Figures 1 and 2 shows the simulation results for the cooling rates 0.05 °C/τ and 0.01°C/τ, with the spatial distributions of the ice crystal, temperature and solute concentration in columns from left to right, respectively. Without lowering the temperature inside the sample, Figure 1 shows that fast cooling from the outside at 0.05 degree/tau lowers the temperature of the outer edge of the phantom locally and ice crystals was observed. At first, the occurrence of new ice nucleus is seen to be small but ice crystal growth was observed along the process. The presence of generation of heat of solidification (middle) and concentration of solute (right) around the growing ice crystal, a new ice nucleus formed away from it. However, when the rate of cooling is slow (see Figure 2), the temperatures in the inner and outer parts of the sample are substantially the same, hence fibrous ice crystals are observed to form within the sample.

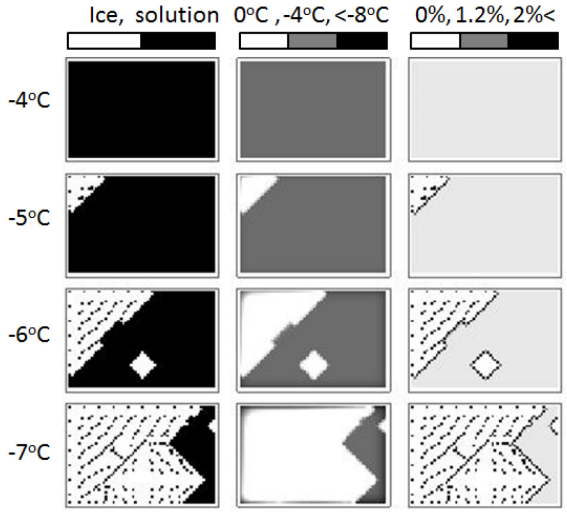

Fig.1 Spatial distribution of ice crystal (left), temperature (center) and solute concentration (right) under cooling rate of 0.05 degree/ tau. Gray scales are put on the top as indicators.

With high cooling rate as shown in Figure 1, the temperature of the inner part of the sample is

insufficiently low due to the generated heat of solidification of the growing ice crystal from the outer part. As the ice nuclei forms, solute concentration is distributed in the liquid part of the sample. The temperature and solute concentration in the ice crystal interface are necessarily lower, which provides more possibility for ice nuclei to form. Hence, ice crystals can spread in bulk from the outer part. However, when the cooling rate is low (see Figure 2), the temperature of the inner part of the sample is low despite the presence of heat of solidification released during the formation of ice nuclei near the outer edge. Fibrous ice crystals visibly grow at low concentration regions away from the interface of the growing ice crystal in the outer edge. As the internal temperature becomes equal or higher than the freezing point, fibrous ice crystals grow within the sample, however, external cooling (-6 ~ -7) ℃ limits this process as ice nucleation and crystal growth were observed from the outer edge.

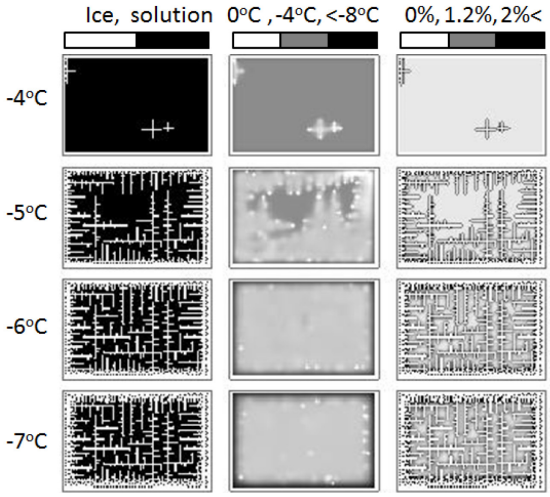

Fig.2 Spatial distribution of ice crystal (left), temperature (center) and solute concentration (right) under cooling rate of 0.01 degree/ tau. Gray scales are put on the top as indicators.

3.2 MRI Measurement

The behavior of the ice crystal growth after breaking the super cooling condition of the outer region of the phantom was investigated. The phantom was immersed in a cold liquid bath set at -8 ℃, and super cooling was achieved in both inner and outer regions. Figure 3 shows the time courses of the temperature in both inner and outer regions while it is immersed in the cold bath. The outer region temperature dropped at around -7 ℃ but showed a sharp increase to 0℃ when the super cooling condition of the outer region was eliminated by hitting the outer wall of the phantom. Breaking the super cooling condition of the outer region generated rapid ice nucleation and the sharp increase in temperature to 0 ℃ is associated with the latent heat of solidification released when fine ice crystals were formed. After breaking the super cooling condition of the outer region, the temperature in the inner region increased slowly and reached to 0 ℃ after 20 minutes. The outer region can be physically observed as cloudy and ice crystals were found to be sticking on the outer wall of the inner region. It is considered that the ice layer on the outer walls of the inner region thickened as the temperature of the inner regions rose up to 0 ℃.

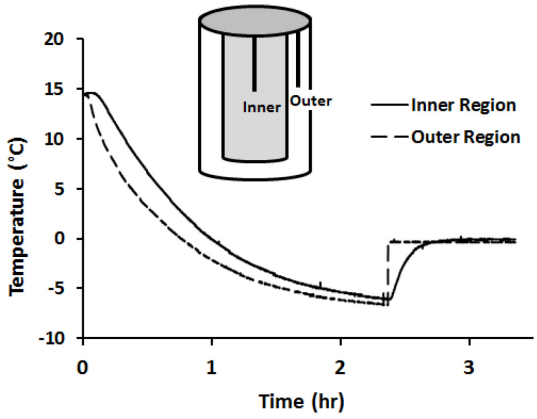

Fig.3 Time courses of temperatures in inner and outer regions of a phantom with cylindrical double layer structure after soaking in the bath at -8 degree.

The ice crystal growth process in the phantom was investigated in detail using MRI measurement (Figure 4). For calibration and comparison purposes, the signal strength for silicone oil is shown (circles under the phantom). The brightness of the image is proportional to the signal strength. Due to the very short relaxation time, the signal from ice crystal decays before signal acquisition and only the signal from water can be observed. Accordingly, the brightness of the image is proportional to the ratio between liquid water and ice crystals and the black region in MRI is corresponding to the part in sample with no liquid water. In the MRI image 3 min after the breaking of supercoiling condition, the outer region in the phantom was slightly darker compared to the inner region of pure liquid water, showing that the outer region was a mixture of fine ice crystals and liquid water. The region with 3 mm thickness from the outside wall was bright because the fine ice crystals were melt by heat from outside (room temperature). At this time, the thickness of black circle between inner and outer regions was about 2 mm. On the other hand, the thickness in the MRI after 1.5 hours was 1 mm corresponding to that of

the outer container. These results show that a layer of bulk ice with thickness of about 1mm formed after 3min. After that, the black circle gradually thickened with the laps time accompanying the melting from outside and become 3mm after 30 min. And after 1 hour, the fine crystals in the outer region disappeared and the back circle thinned. As shown here, MRI measurements confirmed the growth of the bulk ice crystal on the outer wall of the inner region of the phantom.

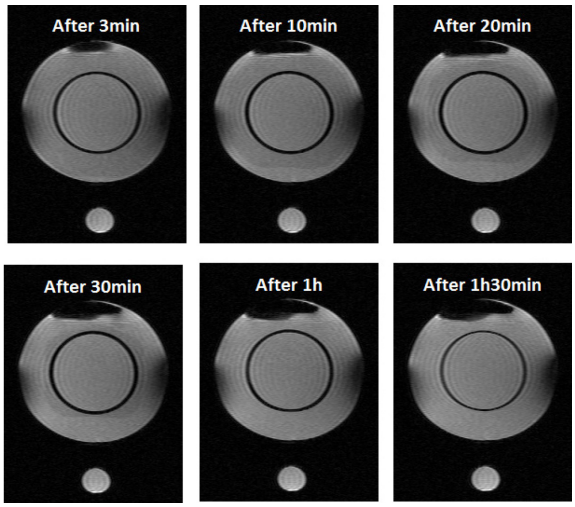

Fig.4 Changes of MRI of the phantom after breaking super-cooling state.

4. Conclusions

Numerical simulations for the formation of ice nucleus and ice crystal growth after breaking the super cooling condition in a substrate solution have been performed. When the cooling rate is high, the ice nucleus is generated from the outer edge and grows in bulk therefrom. On the other hand, when the cooling rate is low, fibrous ice crystals grow within the sample in addition to the bulk ice crystals that grow from the outer edge. MRI measurements show the formation and growth of the bulk ice crystal in the interface between the inner and outer layers of the phantom. After breaking the super cooling condition of the outer layer, its temperature abruptly increased to 0 ℃ and formation of fine ice crystals within the outer layer occurred simultaneously. The inner layer remained in the liquid state as its temperature gradually increased to 0 ℃.

Acknowledgment

This study was conducted as part of the "high-value-added promotion of the Tohoku district fisheries resources using advanced refrigeration technology (technology development leading to the creation of new industries)", Tohoku Marine Science Project. In addition, numerical simulation was carried out with a support of Grant-in-aid by Fuji Science and Technology Foundation.

Reference

1) Fennema, O. “Low-temperature reservation foods and living matter”,1973. Marcel Dekker, Inc., New York, pp. 160-161.
2) Chassagne-Berces, S. et al., Changes in texture, cellular structure and cell wall composition in apple tissue as a result of freezing. *Food Research International*, 2009, **42**(7), pp.788–797.
3) Ando,H., Fukuoka,M., Miyawaki,O., Suzuki,T., Damage evaluation on freeze-thawing process of food by using NMR, *Trans. of the JSRAE*, 2006, **23**, pp.305-312. (in Japanese.)
4) Chow, C. et al., Effect of freezing and thawing on the discoloration of tuna meat. *Nippon Suisan Gakkaishi,* 1988, **54**(4), pp.639–648.
5) Aydin, I. & Gokoglu, N., Effects of temperature and time of freezing on lipid oxidation in anchovy (Engraulis encrasicholus) during frozen storage. *European Journal of Lipid Science and Technology*, 2014, **116**(8), pp.996–1001.
6) Hashizume, K., The Review of “Kohri-tofu”; Japanese traditional dried food (Kohri-tofu no hanashi), *Kagaku to Seibutsu*, 1977, **15**(5), pp. 301-308 (in Japanese).
7) Fuchigami, M., Teramoto, A. & Jibu, Y., Texture and structure of pressure-shift-frozen agar gel with high visco-elasticity. *Food Hydrocolloids*, 2006, **20**. pp.160–169.
8) Kiani, H. & Sun, D., Water crystallization and its importance to freezing of foods : A review. *TIFS*, 2011, **22**(8), pp.407–426.
9) Woinet, B. et al., Experimental and theoretical study of model food freezing. Part II. Characterization and modelling of the ice crystal size. *Journal of Food Engineering*, 1988, **35**(98), pp.395–407.
10) Chevalier, D., Le Bail, A., and Ghoul, M., Freezing and ice crystals formed in a cylindrical food model: part1.Freezing at atmospheric pressure, *Journal of Food Engineering*, 2000, **46**(4), pp. 277-285.
11) Petzold, G., Aguilera, J.M., Ice morphology: Fundamentals and technological applications in foods. *Food Biophysics*, 2009, **4**(4), pp.378–396.
12) Miyawaki, O., Abe, T., and Yano, T., Freezing and ice structure formed in protein gels, *Bioscience, Biotechnology, and Biochemistry*, 1992, **56**(6), pp. 953-957.
13) Simoyamada, M., Tomatsu, K., and Watanabe, K., Effect of precooling step on formation of soymilk freeze-gel, *Food science and technology research*, 1999, **5** (3),pp. 284-288.
14) O’Brien, F.J. et al., Influence of freezing rate on pore structure in freeze-dried collagen-GAG scaffolds. Biomaterials, 2004, **25**(6), pp.1077–1086.
15) Kobayashi, R., Kanesaka, N., Watanabe, M., Suzuki, T., Effect of the breaking temperature of supercooling on ice characteristics and drip loss of foods in supercooled freezing method, *Trans. of the JSRAE*, 2014, **31**, pp. 297-303.(in Japanese)